A phenotypic small-molecule screen identifies halogenated salicylanilides as inhibitors of fungal morphogenesis, biofilm formation and host cell invasion

Carlos Garcia[1], Anaïs Burgain[1], Julien Chaillot[1], Émilie Pic[1], Inès Khemiri[1] and Adnane Sellam[1,2,3]

[1] CHU de Québec Research Center (CHUQ), Université Laval, Quebec City, QC, Canada

[2] Department of Microbiology, Infectious Disease and Immunology, Faculty of Medicine, Université Laval, Quebec City, QC, Canada

[3] Big Data Research Centre (BDRC-UL), Université Laval, Faculty of Sciences and engineering, Quebec City, QC, Canada

* Corresponding authors:
Prof. Adnane Sellam, Université Laval, CHU de Québec Research Center (CHUL), RC-709, 2705 Laurier Blvd, Quebec, QC, Canada G1V 4G2. Tel: (1) 418 525 4444 ext. 46259. E-mails: adnane.sellam.1@ulaval.ca and adnane.sellam@gmail.com

Abstract

A poorly exploited paradigm in the antimicrobial therapy field is to target virulence traits for drug development. In contrast to target-focused approaches, antivirulence phenotypic screens enable identification of bioactive molecules that induce a desirable biological readout without making *a priori* assumption about the cellular target. Here, we screened a chemical library of 678 small molecules against the invasive hyphal growth of the human opportunistic yeast *Candida albicans*. We found that a halogenated salicylanilide (N1-(3,5-dichlorophenyl)-5-chloro-2-hydroxybenzamide) and one of its analog, Niclosamide, an FDA-approved anthelmintic in humans, exhibited both antifilamentation and antibiofilm activities against *C. albicans* and the multi-resistant yeast *C. auris*. The antivirulence activity of halogenated salicylanilides were also expanded to *C. albicans* resistant strains with different resistance mechanisms. We also found that Niclosamide protected the intestinal epithelial cells against invasion by *C. albicans*. Transcriptional profiling of *C. albicans* challenged with Niclosamide exhibited a signature that is characteristic of the mitochondria-to-nucleus retrograde response. Our chemogenomic analysis showed that halogenated salicylanilides compromise the potential-dependant mitochondrial protein translocon machinery. Given the fact that the safety of Niclosamide is well established in humans, this molecule could represent the first clinically approved antivirulence agent against a pathogenic fungus.

Introduction

86
87
88   *Candida albicans* is an ascomycete fungus that is an important commensal and
89 opportunistic pathogen in humans. Systemic infections resulting primarily from this yeast and
90 the filamentous fungus, *Aspergillus fumigatus,* are associated with mortality rates of 50% or
91 greater despite current therapies [1-3]. Therapeutic options are limited to treatment with mainly
92 three antifungal classes, namely polyenes, azoles and echinocandins [4]. These compounds target
93 the specific fungal biological process of ergosterol metabolism (azoles and polyenes) and cell
94 wall β-1,3-glucan synthesis (echinocandins). However, these drugs have serious side effects such
95 as nephrotoxicity and/or create complications such as resistance and interactions with other
96 commonly prescribed drugs. There are currently a limited number of novel antifungal molecules
97 on the drug discovery pipelines and most of them target the same cellular processes as azoles and
98 echinocandins [5-7]. Thus, these molecules will most likely face the same limitations in term of
99 resistance and toxicity. These considerations highlight the urgent need to identify novel targets
100 and strategies for antifungal therapies
101
102 The pathogenicity of *C. albicans* is mediated by different factors such as invasive filamentation,
103 biofilm formation and the ability to escape the immune system [4]. A relatively new but poorly
104 exploited paradigm in the antimicrobial therapy field is to target virulence traits for drug
105 development [8,9]. In contrast to target-focused approaches, phenotypic screens enable
106 identification of bioactive molecules that induce a desirable biological readout without making *a*
107 *priori* assumption about the cellular target. Additionally, compounds identified by phenotypic
108 screens are by definition cell permeable and engage their target with sufficient affinity. Taking
109 into consideration the commensal lifestyle of *C. albicans*, suppressing its growth in different
110 niches inside the host will perturb the microbial flora equilibrium and lead to other opportunistic
111 infections [10]. Specific inhibition of fungal virulence determinants without affecting commensal
112 growth represents thus an attractive approach.
113
114 *C. albicans* is a polymorphic fungus that are able to reversibly shift to different morphologies
115 including yeast, pseudohyphae and true hyphae forms. Hyphae are long tubular cells that are
116 associated with the invasion of organs and tissues of the human host during Candidemia
117 episodes.
118 In addition to ensuring a physical force required to penetrate host cells, the hyphae state is
119 characterized by an enhanced adhesiveness and allow to the fungal cells to escape the from
120 phagocytes and to conquer niches where nutrient conditions are not limiting [11]. Furthermore,
121 even if hyphae are not essential for the formation of *C. albicans* biofilms, they are determinant
122 for the compression strength and the resistance to mechanical dislocation of this highly resistant
123 growth lifestyle [12]. Thus, antivirulence therapy based on molecules that inhibit hyphae formation
124 could have substantial benefits on managing fungal infections. Moreover, antivirulence agents
125 might provide an alternative strategy to circumvent antifungal resistance by disarming fungal
126 resistant pathogens from their virulence factors [13].
127
128 Proof of principle for this concept has been demonstrated in different investigations [14-19]. Fazly
129 *et al.* characterized a small molecule called filastatin that inhibits *C. albicans* filamentation,
130 adhesion and virulence [15], yet, the molecular mechanism by which this molecule acts remain
131 elusive. Recently, screening of small molecules that are being clinically tested for different

132 pathologies identified two antifilamentation compounds that also perturbed endocytosis [16].
133 However, these compounds were also found to inhibit the commensal yeast growth at the
134 effective antifilamentation concentrations.
135
136 In this study, we screened a chemical library of 678 small molecules that were preselected for
137 bioactivity in the budding yeast *S. cerevisiae* and have well-balanced hydrophilic-lipophilic
138 properties allowing the crossing of both the hydrophilic fungal cell wall and the lipophilic
139 membrane. We found that N1-(3,5-dichlorophenyl)-5-chloro-2-hydroxybenzamide (TCSA: Tri-
140 Chloro-Salicyanilide, for simplified nomenclature), a halogenated salicylanilide, was a potent
141 antifilamentation molecule and inhibited also biofilm formation of both *C. albicans* and the
142 multi-resistant yeast *C. auris*. The TCSA analog, Niclosamide, that is an FDA-approved
143 anthelmintic agent, exhibited a similar anti-filamentation and anti-biofilm activities and
144 conferred a significant protective activity to intestinal epithelial cells against fungal invasion.
145 Both genome-wide transcriptional profiling and chemical-genetic approach were used to gain
146 insight into the mechanism of action associated with the antivirulence activity of the halogenated
147 salicylanilides (HSA). We found that HSA-mediated antivirulence activity is likely related to the
148 perturbation of the fungal mitochondrial protein import machinery.
149

Results
Phenotypic screening of yeast-bioactive small molecules for inhibition of hyphal growth
152 To identify small molecules with antivirulence properties the yeast bioactive small molecule
153 library [20] was screened for compounds that inhibit hyphal formation (**Fig. 1A**). Compounds of
154 this chemical library were preselected for bioactivity in *S. cerevisiae* and have well-balanced
155 hydrophilic-lipophilic properties allowing the crossing of both the hydrophilic fungal cell wall
156 and the lipophilic membrane. *C. albicans* cells were grown in 96-well under hyphae-promoting
157 conditions (SC-10% fetal bovine serum (FBS)) for 3h at 37 °C in the presence of the bioactive
158 compounds. The ability of each compounds to inhibit *C. albicans* SC5314 strain morphogenesis
159 was assessed by imaging each well using the high-content microscope Cytation 5. This primary
160 screen identified 93 molecules with anti-filamentation activity at 100μM (70-80% of *C. albicans*
161 cells with no germ tubes). A total of 50 promiscuous molecules with chemical structures similar
162 to pan assay interference compounds (PAINS) associated with antifungal activity [21] were
163 removed from the hit list of the primary screen. Inhibition of filamentation could be associated
164 with the fact that small molecules are very toxic which might systematically alter all
165 developmental process of a fungal cell such as morphogenesis. To rule out cytotoxic molecules
166 that impaired growth *per se*, the 43 retained hits were assayed for their ability to inhibit growth
167 of yeast cells growing at 30°C. Through this process, a subset of five molecules were selected
168 which were then assayed for their potency using a quantitative dose-response filamentation
169 inhibition assay. Among the five hits, we found two molecules that had a significant effect on
170 filamentous growth at pharmacological concentrations of 1-10μM (data not shown). The effect
171 of this compounds on *C. albicans* filamentation were confirmed using a new batch of powders
172 from different suppliers (**Fig. 1B-C**).
173
174 Compound #1 (N1-(3,5-dichlorophenyl)-5-chloro-2-hydroxybenzamide or TCSA) is a
175 halogenated form of salicylanilide scaffold. Salicylanilides are widely used as antiparasitic
176 veterinary drugs against helminths and ectoparasites [22]. The salicylanilide Niclosamide (5-
177 chloro-salicyl-(2-chloro-4-nitro) anilide) was approved by the FDA to treat tape worm infection

4

178 in humans [23] and has been recently shown to have anti-cancer and anti-diabetic activities [24,25].
179 Recently, HSA including Niclosamide and Oxyclozanide were repurposed as alternative
180 antibiotic therapy against clinical resistant isolates of *Staphylococcus aureus* [26]. The compound
181 #2 (3-Chloro-aryl(benzofuran-2-yl) ketoxime) had chemical features with previously described
182 biological activities. This compound had both oxime and benzofuran residues that are associated
183 with the antifungal activity of many molecules [27-32]. Derivatives of compound #2 were also
184 shown to be active against *C. albicans* by targeting the N-myristoyltransferase, Nmt1 [33,34]. While
185 in our conditions this molecule had a slight effect on the growth of the yeast form of *C. albicans*
186 (10% of inhibition at 1mM), other studies using different growth medium (RPMI) had shown a
187 strong growth reduction at 15µM [31]. Based on this, we decided to focus our downstream
188 investigation on compound #1.

189 **TCSA and Niclosamide inhibit *C. albicans* filamentation without affecting the commensal**
190 **yeast growth**
191 Commercially available HSA analogs 3-12 were purchased and tested on both growth and
192 filamentation (**Fig. 2A**). With the exception of Niclosamide (compound #6), all tested
193 salicylanilide derivatives impaired the growth of *C. albicans* at concentration of 20µM (> 50%
194 inhibition of the growth as compared to the control) (**Fig. 2B**). Interestingly, the salicylanilide
195 scaffold alone had a strong effect on the fungal growth, suggesting that halogenation potentiates
196 the antifilamentation rather than yeast antigrowth effect of TCSA and Niclosamide. Both TCSA
197 and Niclosamide have no significant impact on the growth of the yeast form (**Fig. 3A-B**). At
198 50µM, TCSA inhibited hyphae elongation by 90%, as compared to the control, while
199 Niclosamide abolished completely *C. albicans* filamentation (**Fig. 3C-D**).

201 Since the yeast-to-hyphae transition is triggered by different environmental cues, the
202 antifilamentation effect of TCSA and Niclosamide was also tested and confirmed using other
203 hyphae-promoting media. In RPMI medium, both compounds were effective at concentrations
204 similar to those in SC supplemented with 10% FBS (**Fig. 3E**). Interestingly, in Spider, N-
205 acetylglucosamine (GlcNAc) and Lee's media the antifilamentation activity of TCSA and
206 Niclosamide were enhanced and a complete abolition of the *C. albicans* hyphal growth were
207 perceived at concentration ranging from 0.5 to 5µM (**Fig. 3F-I**). Both TCSA and Niclosamide
208 exhibited antifilamentation activity on other non-*albicans* Candida species including *C.*
209 *dubliniensis* and *C. tropicalis* (data not shown).

211 **TCSA and Niclosamide inhibit *C. albicans* biofilm formation**
212 The effect of the two HSA were also assessed on *C. albicans* biofilm, a highly resistant sessile
213 growth lifestyle associated with the contamination of medical devices. Niclosamide and TCSA
214 impaired considerably the ability of *C. albicans* to establish biofilms (**Fig. 4A-B**). Antibiofilm
215 activity were noticed at 1µM (12% inhibition) and 5µM (15% inhibition) for TCSA and
216 Niclosamide, respectively. Both compounds were active on the biofilm of the emerging multi-
217 drug resistant yeast, *C. auris,* and their inhibitory effect was perceived at 1µM (**Fig. 4C-D**). For
218 both *Candida* species, biofilm inhibition was greater with TCSA as compared to Niclosamide.

220 **Niclosamide and TCSA attenuate damage of intestinal epithelial cells caused by *C. albicans***
221 Since Niclosamide and TCSA inhibited the formation of invasive hyphae, we wanted to check
222 whether it conferred a protective activity for host cells against fungal invasion. *C. albicans*-
223 mediated damage of the human colon epithelial HT-29 cells was quantified based on the LDH

224 release assay in cells treated or not with different concentrations of the two HSA. Our data
225 showed clearly that both antifilamentation compounds significantly reduced, but not completely
226 abolished, the damage to HT-29 enterocytes (**Fig. 4E**). The protective effect was perceived at
227 40µM of either Niclosamide or TCSA (~ 20% reduction of enterocyte invasion). At
228 concentration ≥100µM, Niclosamide and TCSA attenuated HT-29 cell damage by 63% and 49%,
229 respectively.
230
231 **Niclosamide induces retrograde response in *C. albicans***
232 To gain insight into the mechanism of action associated with the antifilamentation effect of HSA,
233 transcriptional profiling was undertaken on cells grown under hyphae-stimulating conditions in
234 the presence of 50µM of Niclosamide. Gene ontology analysis showed that transcripts related to
235 drug transport and, carbohydrate, trehalose and glyoxylate metabolisms were induced while
236 genes of cell wall, filamentation and lipid metabolism including ergosterol (*ERG6*, *ERG25*,
237 *CYB5, NDT80*), sphingolipids (*LCB2*, *FEN1*, *LAC1*) and phosphoglycerides (*AYR1*, *CHO2*,
238 *PEL1*, *EPT1*, *YEL1*, *DGK1*) were downregulated (**Table 1**). We also found that genes encoding
239 different proteins that control the activity of different protein kinases such as those modulating
240 cell cycle progression (*CLN3*, *CLG1*, *SOL1*, *CIP1*) were repressed in response to Niclosamide.
241 Gene expression alteration of eight genes including four upregulated (*ICL1*, *MLS1*, *MDR1*,
242 *GDH2*) and four downregulated (*ZRT2*, *ERG25*, *LAC1*, *CDC47*) transcripts was confirmed using
243 qPCR (**Table S1**).
244
245 Of note, transcripts of the isocitrate lyase, *ICL1*, and the malate synthase, *MLS1*, both key
246 enzymes of glyoxylate cycle were highly induced (46- and 13-fold induction for *ICL1* and *MLS1*,
247 respectively) (**Fig. 5A and Table S2**). The glyoxylate cycle is an anaplerotic pathway of the
248 tricarboxylic acid (TCA) cycle that allows assimilation of carbon from C_2 compounds by
249 bypassing the CO_2-generating steps of the TCA cycle. Both Icl1 and Mls1 enzymes are
250 perxisomal, unique to the glyoxylate route and are not shared with the tricarboxylic acid (TCA)
251 cycle [35,36]. Activation of those genes in response to Niclosamide suggests a metabolic
252 reconfiguration where acetyl-CoA is supplied by the glyoxylate cycle instead of the TCA cycle,
253 which might be compromised (**Fig. 5A**). This transcriptional signature is characteristic of the
254 retrograde (RTG) response, which is a mitochondria-to-nucleus signaling that cells activates as a
255 cytoprotective mechanism to compensate for mitochondrial dysfunctions [37]. Another supportive
256 evidence of the TCA cycle failure, is reflected by the activation of genes that mediate other
257 anaplerotic reactions to supply the TCA cycle with intermediates from alternative pathways. This
258 includes the cytoplasmic pyruvate carboxylase enzyme, Pyc2, that converts the pyruvate to
259 oxaloacetate. Transcript level of the glutamate dehydrogenase, Gdh2, that degrades glutamate to
260 ammonia and alpha-ketoglutarate, were also induced (2.67-fold change), however, the levels of
261 induction were not consistent enough ($p = 0.21$) for it to pass the threshold of statistical
262 significance.

263 Activated transcripts were also enriched in genes encoding many proteins with oxidoreductase
264 activity which might reflect a compensatory response to reoxidize the NADH as a consequence
265 of TCA and mitochondrial electron transport failures. Reactivation of glycolytic regulatory genes
266 *PFK26* and *PFK27* suggests also an adaptation to the drop of the intracellular level of ATP as a
267 result of mitochondrial dysfunction. The strong upregulation of the alternative oxidase transcript,
268 Aox2 (31.5-fold induction), emphasizes that *C. albicans* cells might use this alternative electron

6

269   transport systems to bypass the lack of mitochondrial electron transport. Taken together, the
270   Niclosamide-transcriptional signature is reminiscent of cells experiencing an RTG response as a
271   consequence of impaired mitochondrial activity.

Antifilamentation activity of Niclosamide and TCSA against *C. albicans* azole-resistant strains

274   In response to Niclosamide, *C. albicans* cells induced the expression of transporters such as Cdr1
275   and Mdr1 that are a key determinant of antifungal clinical resistance in this human pathogen [38-40].
276   This reflect that *C. albicans* is trying to expel Niclosamide through efflux process. This prompt
277   us to check whether antifungal resistance mediated by efflux process might bypass the
278   antifilamentation effect of HSA. Both Niclosamide and TCSA were tested on clinical strains for
279   which azole resistance is mediated by *MDR1* (strain 6692) and *CDR1* (strain 5674)
280   overexpression. As shown in **Fig. 5B-C**, the antifilamentation effect of the two salicylanilides on
281   these two resistant isolates was similar to that noticed for the SC5314 sensitive clinical strain.
282   This emphasizes that Niclosamide and TCSA could be used to compromise *C. albicans*
283   filamentation of both azole-sensitive and resistant strains.

Niclosamide and TCSA alter the mitochondrial membrane potential

285   In the budding yeast, RTG response is triggered by the loss of mitochondrial membrane potential
286   ($\Delta\Psi$m) as a consequence of mitochondria dysfunction [41]. Thus, Niclosamide or TCSA might
287   induce RTG in *C. albicans* by promoting the perturbation of the $\Delta\Psi$m. Change in $\Delta\Psi$m was
288   quantitatively assessed using JC-1, a green fluorescent potentiometric dye that shifts to red
289   fluorescence as a consequence of $\Delta\Psi$m. *C. albicans* cells treated with either Niclosamide or
290   TCSA exhibited a collapse of the $\Delta\Psi$m which was obvious at the concentration of 5µM (**Fig.
291   5D**). The effect of both HSA on the failure of $\Delta\Psi$m was also confirmed using the MitoTracker
292   dye that stains and accumulate in mitochondria dependently on $\Delta\Psi$m [42] (**Fig. 5E**). These data
293   suggest that both HSA induce RTG response in *C. albicans* as consequence of the alteration of
294    $\Delta\Psi$m.

295

Mutants of the mitochondrial protein import machinery are required for Niclosamide tolerance and filamentation

298   Chemical-genetic assays such as the haploinsufficient profiling (HIP) is a powerful tool that has
299   been widely used to uncover the mechanism of action (MoA) of many bioactive compounds [43-46].
300   The principle of the HIP assay is based on the fact that decreased dosage of a drug target gene in
301   a heterozygous mutant can result in increased drug sensitivity. To investigate the MoA of the
302   HSA associated with their antifilamentation activity, we mined the data of HIP experiments
303   performed in the yeast model *S. cerevisiae* in two resource studies [47,48]. Hoepfner *et al.* [47] has
304   performed HIP assay for Niclosamide while other analogs similar to HSA were investigated
305   using the same approach by Corey Nislow' group [48]. To gain a consensual knowledge into the
306   MoA of HSA, common hits identified by HIP assay of these related compound were identified
307   by Venn diagram that revealed *mge1*/*MGE1* mutant as unique common hit for the five HSA (**Fig.
308   6A**).

309

310   Mge1 is a nucleotide release factor for the mitochondrial heat shock protein 70, Ssc1 that acts by
311   facilitating the release of ADP from Ssc1 [49]. This process is essential for the import complex to
312   translocate nuclear-encoded proteins to their final mitochondrial destination. Both Mge1 and

313 Scc1 are components of the Tim23-Tim17 import motor complex that mediates the translocation
314 of proteins through the inner mitochondrial membrane [50]. The sensitivity of *C. albicans*
315 heterozygous mutants of TIM23 complex including *tim23/TIM23*, *tim17/TIM17, tim50/TIM50,*
316 *ssc1/SSC1* and *mge1/MGE1* was tested toward high concentration of Niclosamide (200µM).
317 While the WT parental strain had no discernable growth defect, all tested mutants were sensitive
318 when exposed to Niclosamide (**Fig. 6B**). The Niclosamide-induced haploinsufficiency of the
319 TIM23 complex suggests that the *C. albicans* translocase machinery of the inner mitochondrial
320 membrane is required to tolerate Niclosamide and/or might be a target of this HSA.
321
322 In opposite to *S. cerevisiae, MGE1* is not essential in *C. albicans* [51]. As for the heterozygous
323 mutant strain, the conditional homozygous mutant *mge1/pTeT-MGE1* under repressive condition
324 (100µg/mL tetracycline) was also sensitive to Niclosamide (not shown). Furthermore, genetic
325 inactivation of *MGE1* led to a complete filamentation defect which support the hypothesis that
326 this protein might be the target of HSA (**Fig. 6C**).
327
328 **Chemical genetics of hyphal signaling using TCSA and Niclosamide as perturbers**
329 The *C. albicans* morphogenetic switch is controlled by intertwined regulatory circuits that signal
330 different filamentation cues. The RAS/cAMP [52], the MAPK [53] and Ume6/Hgc1 [54] pathways are
331 high hierarchical regulators and signaling hubs that control the filamentation process in *C.*
332 *albicans*. To test whether Niclosamide and TCSA alter *C. albicans* filamentation through these
333 pathways, the effect of the two molecules was assessed in mutants overexpressing *UME6*, *HGC1*
334 and the MAPKKK, *STE11* in addition to the dominant mutant Ras1[G13V]. These mutants
335 constitutively formed hyphae or pseudohyphae which will determine whether antifilamentation
336 molecules act upstream or downstream these pathways. Niclosamide and TCSA blocked *C.*
337 *albicans* filamentation regardless the targeted regulators suggesting that both compounds acted
338 on effectors downstream these signaling pathways (**Fig. 7A-B**).
339
340

Discussion

342
343 Neutralizing the virulence traits of a fungal pathogen represents a promising therapeutic strategy
344 to circumvent antifungal resistance. Regardless the degree of susceptibility or resistance of a
345 fungal strain toward conventional antifungal drugs, antivirulence molecules lead to the silencing
346 of the virulence machinery which in turn inhibits the installation of the infection. Furthermore,
347 antivirulence agents could bypass the undesirable side effects of antimicrobials that kill
348 beneficial commensal fungi including *C. albicans* itself [13]. In the current work, we have
349 repurposed the widely used anthelminthic, Niclosamide and its derivative TCSA as a promising
350 antivirulence compounds that impede both invasive filamentation and biofilm formation in both
351 susceptible and resistant clinical *C. albicans* strains. Currently, the antivirulence paradigm was
352 clinically exploited to manage bacterial virulence factors such as anthrax toxins and botulinum
353 neurotoxin [13]. To our knowledge, and given the fact that the safety of Niclosamide is well
354 established in humans [55], this molecule could represent the first clinically approved antivirulence
355 agent against a pathogenic fungus. Interestingly, this anthelmintic agent was also shown to be
356 affective toward bacterial pathogens as an antivirulence molecules against *Pseudomonas*
357 *aeruginosa* [56] or as an antibiotic against multi-resistant strains of *Staphylococcus aureus* [26]. This

8

358 newly discovered antibacterial and antifungal proprietes would reinforce and maintain the status
359 of Niclosamide as being one of the essential medicines in the list the World Health Organization.
360
361 Here, we uncovered that halogenated salicylanilides represent new chemical scaffolds that
362 impede specifically *C. albicans* virulence without affecting the commensal yeast growth. Future
363 comprehensive structure-guided medicinal chemistry investigations are required to precisely
364 point out the chemical group that lead to this discriminative antivirulence activity. Of note, the
365 non-halogenated salicylanilide scaffold (compound #3) has a strong anti-growth activity against
366 *C. albicans* and suggests that halogenation enhances the antivirulence activity. Halogen bonds
367 are exploited in medicinal chemistry for their steric effect to accommodate a best fitting of a
368 small molecule to occupy the binding site of its target [57]. Our data showed that chlorination was
369 more effective as compared to fluorination (compound #5 and #8) or bromination (compound
370 #11) regarding the antivirulence activity. This might be explained by the fact that, as compared
371 to the other halogens-carbon bonds, C-Cl is more stable which might allow a steady docking on
372 its virulence-related target [57].
373
374 Regarding the mechanism of action, HSA have been associated with the perturbation of a
375 plethora of biological processes in bacteria and parasites. Salicylanilides have been shown to
376 inhibit the two-component regulatory systems, uptake of nutrients and oxidative
377 phosphorylation, and to cause leakage and membrane damage and protein aggregation [58].
378 However, their mechanisms associated with their antifungal or antivirulence activity were not
379 investigated so far. In the current study, the transcriptional signature exhibited by *C. albicans*
380 cells exposed to Niclosamide suggests activation of different anaplerotic metabolic pathways that
381 can sustain the TCA cycle with metabolites such as citrate, succinate and oxaloacetate. This
382 phenomenon, so-called RTG, is most likely triggered in *C. albicans* cells as a consequence of the
383 dissipation of the mitochondrial potential. The HIP assays on cells treated to different HSA
384 uncovered that Mge1 might be a potential target of Niclosamide and TCSA. Indeed, genetic
385 inactivation of Mge1 led to a complete filamentation defect which supports the hypothesis that
386 this protein might be the target of HSA.
387
388 Mge1 is a nucleotide release factor that mediates the release of ADP from the heat shock protein
389 Ssc1 [49]. This process is essential for the mitochondrial import complex to translocate nuclear-
390 encoded proteins to mitochondria. Interestingly, this process is $\Delta\Psi$m-depend which suggests that
391 the collapse of $\Delta\Psi$m mediated by HSA might contribute to the malfunctioning of the
392 mitochondrial import complex and thus compromises protein translocation in the mitochondria
393 [59]. Alternatively, in addition to its role as ADP-ATP recycling factor, Mge1 functions as a co-
394 chaperone in the mitochondrial matrix together with Scc1 and Mdj1 to refold desaturated
395 proteins [60]. Taken together, either protein translocation or refolding functions of Mge1 could be
396 hampered by HSA which in turn lead to the filamentation defect in *C. albicans*.
397
398 While deep investigations are required to validate that Mge1 and/or the mitochondrial protein
399 import complex as a target of HSA, previous elegant investigations in *C. albicans* have shown
400 that many fungal mitochondrial proteins are therapeutic targets for antifungal development [61].
401 Furthermore, Mge1 has been recently shown to be a key regulator of azole susceptibility [62] which
402 make the fungal mitochondria as an attractive organelle target to develop anti-virulence, anti-
403 growth and anti-resistance molecules to manage fungal infection.

9

404
Methods
406
Strains and growth conditions
408 The strains used in the current study are listed and described in **Table 2**. For general propagation,
409 the strains were cultured at 30°C in synthetic complete (SC; 0.67% yeast nitrogen base with
410 ammonium sulfate, 2% glucose, and 0.079% complete supplement mixture) or yeast-peptone-
411 dextrose (YPD; 2% Bacto-peptone, 1% yeast extract, 2% dextrose) media supplemented with
412 uridine (50mg/L).

Screen of the bioactive chemical yeast library
414 To identify small molecules with antifilamentation properties, the yeast bioactive small molecule
415 library from Dr Mike Tyers (University of Montreal) consisting of 678 compounds preselected
416 from the Maybridge collection (Thermo Fisher Scientific) was screened. *C. albicans* SC5314
417 strain cells were grown in 96-well in SC medium supplemented with 10% FBS (Wisent) and one
418 microliter of each compound from the master library plate was dispensed into the assay plate at a
419 final concentration of 100µM. DMSO at 1% (v/v) final concentration was added as control to
420 each assay plate. After an incubation for 3h in the high-content microscope Cytation 5 (BioTek®,
421 Thermo Fisher Scientific), images were taken in each well. Hit from this primary screen were
422 confirmed using new batch of powders ordered separately. Frequent hitters and promiscuous
423 compounds in antifungal discovery pipelines [21] were removed from our hit list. Effect of
424 antifilamentation compounds on the yeast growth of *C. albicans* were assessed as follow:
425 SC5314 strain was grown overnight in YPD medium at 30°C in a shaking incubator at 220 rpm.
426 Cells were then resuspended in fresh SC at an OD_{600} of 0.05. A total volume of 99µl fungal cells
427 was added to each well of a flat-bottom 96-well plate in addition to 1µl of the corresponding
428 stock solution antifilamentation molecules. Plates were incubated in a Sunrise-Tecan plate reader
429 at 30°C with agitation and OD_{600} readings were taken every 10min over 24h. Each experiment
430 was performed in triplicate.

Hyphal growth and biofilm assays
432 An overnight culture of the *C. albicans* strains was used to inoculate a 5mL of fresh YPD at an
433 OD_{600} of 0.05. Cells were grown for 4 h at 30°C under agitation to reach the exponential phase.
434 To induce hypha, the SC5314, 6692 and 5674 strains were grown at 37°C in YPD supplemented
435 with either 10% FBS (Wisent) or 2.5mM N-acetyl-D- glucosamine (Sigma), or in Spider (1%
436 mannitol, 1% nutrient broth, 0.2% K2HPO4) , Lee's [63] or RPMI 1640 (Gibco) media. The
437 filament length of the generated filaments was assessed for at least 100 *C. albicans* cells per
438 sample, and all experiments were performed in triplicate. The effect of HSA on hyphae lengths
439 were presented as box plot using the BoxPlotR web tool [64].

440 Biofilm formation and XTT (2,3-bis(2-methoxy-4-nitro-5-sulfo- phenyl)-2H-tetrazolium-5-
441 carboxanilide) assays were carried out as follow: overnight YPD cultures were washed three
442 times with PBS and resuspended in fresh RPMI 1640 supplemented with L-glutamine (0.3g/L) to
443 an OD_{600} of 0.1. *C. albicans* yeast cells were allowed to attach to a flat-bottom 96-well
444 polystyrene plate for 3h at 37°C in a rocking incubator. After removing non-attached cells by
445 washing 3 time using PBS, fresh RPMI supplemented with HAS was added. The plates were
446 then incubated for 24 hours at 37°C for biofilm formation under agitation at 220 rpm. Each well

447 in the plate was then washed 3 times with PBS and fresh RPMI supplemented with 100μl of
448 XTT-menadione mix (0.5mg/ml XTT in PBS and 1mM menadione in acetone) was added. After
449 3 hours of incubation on dark at 37°C, 80μl of the resulting colored supernatants were used for
450 colorimetric reading at an OD_{490} to assess metabolic activity of biofilms. A minimum of four
451 replicates were at least performed. Biofilm formation for *C. auris* was performed as for *C.*
452 *albicans* with the sole exception that cells were allowed to attach for 6 hours.

Transcriptional profiling
454 Overnight cultures of *C. albicans* strain SC5314 were diluted to an OD_{600} of 0.1 in 100mL of
455 fresh YPD and grown at 30°C until an OD_{600} of 0.65. The culture was divided into two volumes
456 of 50mL where 10% FBS serum was added to induce hyphae formation; one sample was
457 maintained as the control where DMSO was added, and the other treated with Niclosamide at
458 50μM. *Candida* cells were then incubated at 37°C and under agitation at 220 rpm for 15 min.
459 Cells were then centrifuged for 2min at 3,500 rpm, the supernatants were removed, and the
460 samples were quick-frozen and stored at 80°C.

461 RNA extractions, cDNA labelling and microarrays procedures were performed as described by
462 Chaillot *et al.* [65]. Data analysis were carried out using Genespring v.7.3 (Agilent Technologies,
463 Palo Alto, CA). Statistical analysis used Welch's *t*-test with a false-discovery rate (FDR) of 5%
464 and 2-fold enrichment cut-off. Gene ontology (GO) analysis was performed using the Candida
465 Genome Database (CGD) GO Term Finder. The *p*-value was calculated using hypergeometric
466 distribution with multiple hypothesis correction (http://www.candidagenome.org/cgi-bin/
467 GO/goTermFinder) [66]. Descriptions of each *C. albicans* gene in **Table S1** were extracted from
468 CGD database [67].

469 For quantitative real time PCR (qPCR) confirmation, cell cultures and RNA extractions were
470 performed as described for the microarray experiment. cDNA was synthesized from 1μg of total
471 RNA using High-Capacity cDNA Reverse Transcription kit (Applied Biosystems). The mixture
472 was incubated at 25°C for 10min, 37°C for 120min and 85°C for 5min. Then RNAse H (NEB)
473 was added to remove RNA. qPCR was performed using LightCycler 480 Instrument (Roche Life
474 Science) with SYBR Green fluorescence (Applied Biosystems). The reactions were incubated at
475 50°C for 2 min, 95°C for 2min and cycled 40 times at 95°C, 15 s; 54°C, 30 s; 72°C, 1 min. Fold-
476 enrichment of each tested transcripts was estimated using the comparative ΔΔCt method as
477 described by Guillemette *et al.* [68]. To evaluate the gene expression level, the results were
478 normalized using Ct values obtained from Actin (*ACT1*, C1_13700W_A). Primer sequences used
479 for this analysis are summarized in Supplemental Table S3.
480

HT-29 damage assay
482 Damage to the human enterocyte HT-29 (ATCC-HTB-38) was assessed using a lactate
483 dehydrogenase (LDH) cytotoxicity detection kit, which measures the release of LDH in the
484 growth medium as described by Garcia *et al.* [69]. Briefly, enterocytes were plated at 10.000 cells
485 per 96-well in Dulbecco's modified Eagle's medium (DMEM) supplemented with 10% FBS and
486 incubated overnight at 37°C with 5% CO_2. The HT-29 cells were then infected with *C. albicans*
487 SC5314 strain cells with a multiplicity of infection (MOI) of 1:20 (Enterocyte:*C. albicans*).
488 Following 24 hours of incubation, 100μL supernatant was removed from each experimental well

11

489 and LDH activity in this supernatant was determined by measuring the absorbance at 490 nm.
490 Each LDH activity assay was performed in triplicate and at least three independent biological
491 replicates were performed.

Chemical epistasis assay
493 Inhibition assay of ectopically hyphae-grown strains KC753 (*MAL2*-STE11*ΔN*), KC763 (*MAL2*-
494 *UME6*) and KC754 (*MAL2*- *HGC1ΔC*) as well as their control strain KC685 was performed as
495 follow: cells were grown overnight in SC medium where glucose was replaced by 2% raffinose.
496 Overexpression of *UME6*, *STE11* and *HGC1* was ensured by diluting the overnight cultures in
497 fresh SC medium where glucose was replaced by 2% maltose in the presence or not of HSA. The
498 cells were incubated for 5h at 30°C. The DH409 mutant with a hyperactive Ras1 (Ras1^{G13V})
499 allele and the control strain DH545 were allowed to filament in Spider medium at 30°C in the
500 presence of HSA for 2h.

Measurements of mitochondrial membrane potential
502 The mitochondrial membrane potential of *C. albicans* cells was measured using both fluorescent
503 probes, JC-1 and MitoTracker Red CMXRos (ThermoFisher). Exponentially grown *C. albicans*
504 cells were washed twice with PBS and treated or not with different concentrations of either
505 Niclosamide or TCSA for 30 min under hyphae promoting conditions. JC1 and MitoTracker
506 were added to *C. albicans* cells at final concentration of 5 µM and 100 nM, respectively, and
507 cells were incubated at 30°C for 30 min in dark. Cells were then washed twice with PBS to
508 remove residual dyes. Fore JC-1, fluorescence was quantitatively assessed using flow cytometry
509 (BD FACSCanto™) using 10^6 *C. albicans* cells. For the MitoTracker assay, the fluorescence was
510 measured using the Cytation 5 plate reader (BioTek$^®$). Results of JC-1 and MitoTracker assays
511 were measured as the mean of fluorescence intensities of at least three independent experiments.

Acknowledgments

Author Contributions
526 AS designed the experiments. CG, AB, JC, EP, IK and AS performed the experiments and
527 interpreted the data. CG and AS wrote the paper. All authors reviewed the manuscript.

Additional Information
529 **Competing Interests**: The authors declare no competing interests.

530

References

532

533   1   Pfaller, M. A. & Diekema, D. J. Epidemiology of invasive candidiasis: a persistent public health problem. *Clinical microbiology reviews* **20**, 133-163, doi:10.1128/CMR.00029-06 (2007).

536   2   Gudlaugsson, O. *et al.* Attributable mortality of nosocomial candidemia, revisited. *Clinical infectious diseases : an official publication of the Infectious Diseases Society of America* **37**, 1172-1177, doi:10.1086/378745 (2003).

539   3   Pappas, P. G. *et al.* Clinical practice guidelines for the management of candidiasis: 2009 update by the Infectious Diseases Society of America. *Clinical infectious diseases : an official publication of the Infectious Diseases Society of America* **48**, 503-535, doi:10.1086/596757 (2009).

543   4   Shapiro, R. S., Robbins, N. & Cowen, L. E. Regulatory circuitry governing fungal development, drug resistance, and disease. *Microbiology and molecular biology reviews : MMBR* **75**, 213-267, doi:10.1128/MMBR.00045-10 (2011).

546   5   Perfect, J. R. The antifungal pipeline: a reality check. *Nat Rev Drug Discov* **16**, 603-616, doi:10.1038/nrd.2017.46 (2017).

548   6   Wurtele, H. *et al.* Modulation of histone H3 lysine 56 acetylation as an antifungal therapeutic strategy. *Nat Med* **16**, 774-780, doi:10.1038/nm.2175 (2010).

550   7   Raj, S. *et al.* The Toxicity of a Novel Antifungal Compound Is Modulated by Endoplasmic Reticulum-Associated Protein Degradation Components. *Antimicrob Agents Chemother* **60**, 1438-1449, doi:10.1128/AAC.02239-15 (2015).

553   8   Alksne, L. E. & Projan, S. J. Bacterial virulence as a target for antimicrobial chemotherapy. *Curr Opin Biotechnol* **11**, 625-636 (2000).

555   9   Gauwerky, K., Borelli, C. & Korting, H. C. Targeting virulence: a new paradigm for antifungals. *Drug discovery today* **14**, 214-222, doi:10.1016/j.drudis.2008.11.013 (2009).

557   10   Rizzetto, L. & Cavalieri, D. Friend or foe: using systems biology to elucidate interactions between fungi and their hosts. *Trends in microbiology* **19**, 509-515, doi:10.1016/j.tim.2011.07.007 (2011).

560   11   Jacobsen, I. D. *et al.* Candida albicans dimorphism as a therapeutic target. *Expert Rev Anti Infect Ther* **10**, 85-93, doi:10.1586/eri.11.152 (2012).

562   12   Paramonova, E., Krom, B. P., van der Mei, H. C., Busscher, H. J. & Sharma, P. K. Hyphal content determines the compression strength of Candida albicans biofilms. *Microbiology* **155**, 1997-2003, doi:10.1099/mic.0.021568-0 (2009).

565   13   Dickey, S. W., Cheung, G. Y. C. & Otto, M. Different drugs for bad bugs: antivirulence strategies in the age of antibiotic resistance. *Nat Rev Drug Discov* **16**, 457-471, doi:10.1038/nrd.2017.23 (2017).

568   14   Toenjes, K. A. *et al.* Small-molecule inhibitors of the budded-to-hyphal-form transition in the pathogenic yeast Candida albicans. *Antimicrob Agents Chemother* **49**, 963-972, doi:10.1128/AAC.49.3.963-972.2005 (2005).

571 15   Fazly, A. *et al.* Chemical screening identifies filastatin, a small molecule inhibitor of
572   Candida albicans adhesion, morphogenesis, and pathogenesis. *Proceedings of the*
573   *National Academy of Sciences of the United States of America* **110**, 13594-13599,
574   doi:10.1073/pnas.1305982110 (2013).
575 16   Bar-Yosef, H., Vivanco Gonzalez, N., Ben-Aroya, S., Kron, S. J. & Kornitzer, D. Chemical
576   inhibitors of Candida albicans hyphal morphogenesis target endocytosis. *Sci Rep* **7**, 5692,
577   doi:10.1038/s41598-017-05741-y (2017).
578 17   Goffena, J., Toenjes, K. A. & Butler, D. K. Inhibition of Yeast-to-Filamentous Growth
579   Transitions in Candida albicans by a Small Molecule Inducer of Mammalian Apoptosis.
580   *Yeast*, doi:10.1002/yea.3287 (2017).
581 18   Romo, J. A. *et al.* Development of Anti-Virulence Approaches for Candidiasis via a Novel
582   Series of Small-Molecule Inhibitors of Candida albicans Filamentation. *MBio* **8**,
583   doi:10.1128/mBio.01991-17 (2017).
584 19   Vila, T. & Lopez-Ribot, J. L. Screening the Pathogen Box for Identification of Candida
585   albicans Biofilm Inhibitors. *Antimicrob Agents Chemother* **61**, doi:10.1128/AAC.02006-16
586   (2017).
587 20   Ishizaki, H. *et al.* Combined zebrafish-yeast chemical-genetic screens reveal gene-
588   copper-nutrition interactions that modulate melanocyte pigmentation. *Disease models*
589   *& mechanisms* **3**, 639-651, doi:10.1242/dmm.005769 (2010).
590 21   Pouliot, M. & Jeanmart, S. Pan Assay Interference Compounds (PAINS) and Other
591   Promiscuous Compounds in Antifungal Research. *J Med Chem* **59**, 497-503,
592   doi:10.1021/acs.jmedchem.5b00361 (2016).
593 22   Swan, G. E. The pharmacology of halogenated salicylanilides and their anthelmintic use
594   in animals. *J S Afr Vet Assoc* **70**, 61-70 (1999).
595 23   Frayha, G. J., Smyth, J. D., Gobert, J. G. & Savel, J. The mechanisms of action of
596   antiprotozoal and anthelmintic drugs in man. *Gen Pharmacol* **28**, 273-299 (1997).
597 24   Tao, H., Zhang, Y., Zeng, X., Shulman, G. I. & Jin, S. Niclosamide ethanolamine-induced
598   mild mitochondrial uncoupling improves diabetic symptoms in mice. *Nat Med* **20**, 1263-
599   1269, doi:10.1038/nm.3699 (2014).
600 25   Ye, T. *et al.* The anthelmintic drug niclosamide induces apoptosis, impairs metastasis
601   and reduces immunosuppressive cells in breast cancer model. *PLoS One* **9**, e85887,
602   doi:10.1371/journal.pone.0085887 (2014).
603 26   Rajamuthiah, R. *et al.* Repurposing salicylanilide anthelmintic drugs to combat drug
604   resistant Staphylococcus aureus. *PLoS One* **10**, e0124595,
605   doi:10.1371/journal.pone.0124595 (2015).
606 27   Rossello, A. *et al.* Synthesis, antifungal activity, and molecular modeling studies of new
607   inverted oxime ethers of oxiconazole. *J Med Chem* **45**, 4903-4912 (2002).
608 28   Gundogdu-Karaburun, N., Benkli, K., Tunali, Y., Ucucu, U. & Demirayak, S. Synthesis and
609   antifungal activities of some aryl [3-(imidazol-1-yl/triazol-1-ylmethyl) benzofuran-2-yl]
610   ketoximes. *Eur J Med Chem* **41**, 651-656, doi:10.1016/j.ejmech.2005.12.013 (2006).
611 29   Benkli, K. *et al.* Synthesis and antifungal activities of some aryl (3-methyl-benzofuran-2-
612   yl) ketoximes. *Arch Pharm Res* **26**, 202-206 (2003).
613 30   Koca, M. *et al.* Synthesis and antimicrobial activity of some novel derivatives of
614   benzofuran: part 1. Synthesis and antimicrobial activity of (benzofuran-2-yl)(3-phenyl-3-

615   methylcyclobutyl) ketoxime derivatives. *Eur J Med Chem* **40**, 1351-1358,
616   doi:10.1016/j.ejmech.2005.07.004 (2005).
617   31   Demirayak, S. *et al.* Synthesis and antifungal activities of some aryl(benzofuran-2-
618   yl)ketoximes. *Farmaco* **57**, 609-612 (2002).
619   32   Nevagi, R. J., Dighe, S. N. & Dighe, S. N. Biological and medicinal significance of
620   benzofuran. *Eur J Med Chem* **97**, 561-581, doi:10.1016/j.ejmech.2014.10.085 (2015).
621   33   Telvekar, V. N., Kundaikar, H. S., Patel, K. N. & Chaudhari, H. K. 3-D QSAR and Molecular
622   Docking Studies on Aryl Benzofuran-2-yl Ketoxime Derivatives as Candida albicans N-
623   myristoyl transferase Inhibitors. *QSAR & Combinatorial Science* **27**, 1193-1203,
624   doi:10.1002/qsar.200810017 (2008).
625   34   Kawasaki, K. *et al.* Design and synthesis of novel benzofurans as a new class of
626   antifungal agents targeting fungal N-myristoyltransferase. Part 3. *Bioorg Med Chem Lett*
627   **13**, 87-91 (2003).
628   35   Piekarska, K. *et al.* The activity of the glyoxylate cycle in peroxisomes of Candida albicans
629   depends on a functional beta-oxidation pathway: evidence for reduced metabolite
630   transport across the peroxisomal membrane. *Microbiology* **154**, 3061-3072,
631   doi:10.1099/mic.0.2008/020289-0 (2008).
632   36   Dunn, M. F., Ramirez-Trujillo, J. A. & Hernandez-Lucas, I. Major roles of isocitrate lyase
633   and malate synthase in bacterial and fungal pathogenesis. *Microbiology* **155**, 3166-3175,
634   doi:10.1099/mic.0.030858-0 (2009).
635   37   Jazwinski, S. M. The retrograde response: a conserved compensatory reaction to
636   damage from within and from without. *Prog Mol Biol Transl Sci* **127**, 133-154,
637   doi:10.1016/B978-0-12-394625-6.00005-2 (2014).
638   38   Tsao, S., Rahkhoodaee, F. & Raymond, M. Relative contributions of the Candida albicans
639   ABC transporters Cdr1p and Cdr2p to clinical azole resistance. *Antimicrob Agents*
640   *Chemother* **53**, 1344-1352, doi:10.1128/AAC.00926-08 (2009).
641   39   Holmes, A. R. *et al.* ABC transporter Cdr1p contributes more than Cdr2p does to
642   fluconazole efflux in fluconazole-resistant Candida albicans clinical isolates. *Antimicrob*
643   *Agents Chemother* **52**, 3851-3862, doi:10.1128/AAC.00463-08 (2008).
644   40   White, T. C. Increased mRNA levels of ERG16, CDR, and MDR1 correlate with increases in
645   azole resistance in Candida albicans isolates from a patient infected with human
646   immunodeficiency virus. *Antimicrob Agents Chemother* **41**, 1482-1487 (1997).
647   41   Jazwinski, S. M. & Kriete, A. The yeast retrograde response as a model of intracellular
648   signaling of mitochondrial dysfunction. *Front Physiol* **3**, 139,
649   doi:10.3389/fphys.2012.00139 (2012).
650   42   Pendergrass, W., Wolf, N. & Poot, M. Efficacy of MitoTracker Green and CMXrosamine
651   to measure changes in mitochondrial membrane potentials in living cells and tissues.
652   *Cytometry A* **61**, 162-169, doi:10.1002/cyto.a.20033 (2004).
653   43   Baetz, K. *et al.* Yeast genome-wide drug-induced haploinsufficiency screen to determine
654   drug mode of action. *Proceedings of the National Academy of Sciences of the United*
655   *States of America* **101**, 4525-4530, doi:10.1073/pnas.0307122101 (2004).
656   44   Giaever, G. *et al.* Chemogenomic profiling: identifying the functional interactions of
657   small molecules in yeast. *Proceedings of the National Academy of Sciences of the United*
658   *States of America* **101**, 793-798, doi:10.1073/pnas.0307490100 (2004).

659 45 Lum, P. Y. *et al.* Discovering modes of action for therapeutic compounds using a
660   genome-wide screen of yeast heterozygotes. *Cell* **116**, 121-137 (2004).
661 46 Xu, D. *et al.* Genome-wide fitness test and mechanism-of-action studies of inhibitory
662   compounds in Candida albicans. *PLoS pathogens* **3**, e92,
663   doi:10.1371/journal.ppat.0030092 (2007).
664 47 Hoepfner, D. *et al.* High-resolution chemical dissection of a model eukaryote reveals
665   targets, pathways and gene functions. *Microbiol Res* **169**, 107-120,
666   doi:10.1016/j.micres.2013.11.004 (2014).
667 48 Lee, A. Y. *et al.* Mapping the cellular response to small molecules using chemogenomic
668   fitness signatures. *Science* **344**, 208-211, doi:10.1126/science.1250217 (2014).
669 49 Liu, Q., D'Silva, P., Walter, W., Marszalek, J. & Craig, E. A. Regulated cycling of
670   mitochondrial Hsp70 at the protein import channel. *Science* **300**, 139-141,
671   doi:10.1126/science.1083379 (2003).
672 50 Demishtein-Zohary, K. & Azem, A. The TIM23 mitochondrial protein import complex:
673   function and dysfunction. *Cell Tissue Res* **367**, 33-41, doi:10.1007/s00441-016-2486-7
674   (2017).
675 51 O'Meara, T. R. *et al.* Global analysis of fungal morphology exposes mechanisms of host
676   cell escape. *Nat Commun* **6**, 6741, doi:10.1038/ncomms7741 (2015).
677 52 Feng, Q., Summers, E., Guo, B. & Fink, G. Ras signaling is required for serum-induced
678   hyphal differentiation in Candida albicans. *J Bacteriol* **181**, 6339-6346 (1999).
679 53 Csank, C. *et al.* Roles of the Candida albicans mitogen-activated protein kinase homolog,
680   Cek1p, in hyphal development and systemic candidiasis. *Infect Immun* **66**, 2713-2721
681   (1998).
682 54 Wang, Y. Hgc1-Cdc28-how much does a single protein kinase do in the regulation of
683   hyphal development in Candida albicans? *J Microbiol* **54**, 170-177, doi:10.1007/s12275-
684   016-5550-9 (2016).
685 55 Andrews, P., Thyssen, J. & Lorke, D. The biology and toxicology of molluscicides,
686   Bayluscide. *Pharmacol Ther* **19**, 245-295 (1982).
687 56 Imperi, F. *et al.* New life for an old drug: the anthelmintic drug niclosamide inhibits
688   Pseudomonas aeruginosa quorum sensing. *Antimicrob Agents Chemother* **57**, 996-1005,
689   doi:10.1128/AAC.01952-12 (2013).
690 57 Hernandes, M. Z., Cavalcanti, S. M., Moreira, D. R., de Azevedo Junior, W. F. & Leite, A.
691   C. Halogen atoms in the modern medicinal chemistry: hints for the drug design. *Curr*
692   *Drug Targets* **11**, 303-314 (2010).
693 58 Kratky, M. & Vinsova, J. Salicylanilide ester prodrugs as potential antimicrobial agents--a
694   review. *Curr Pharm Des* **17**, 3494-3505 (2011).
695 59 Dudek, J., Rehling, P. & van der Laan, M. Mitochondrial protein import: common
696   principles and physiological networks. *Biochim Biophys Acta* **1833**, 274-285,
697   doi:10.1016/j.bbamcr.2012.05.028 (2013).
698 60 Kubo, Y. *et al.* Two distinct mechanisms operate in the reactivation of heat-denatured
699   proteins by the mitochondrial Hsp70/Mdj1p/Yge1p chaperone system. *J Mol Biol* **286**,
700   447-464 (1999).
701 61 Li, D. & Calderone, R. Exploiting mitochondria as targets for the development of new
702   antifungals. *Virulence* **8**, 159-168, doi:10.1080/21505594.2016.1188235 (2017).

703　62　Demuyser, L. *et al.* Mitochondrial Cochaperone Mge1 Is Involved in Regulating
704　　　Susceptibility to Fluconazole in Saccharomyces cerevisiae and Candida Species. *MBio* **8**,
705　　　doi:10.1128/mBio.00201-17 (2017).
706　63　Lee, K. L., Buckley, H. R. & Campbell, C. C. An amino acid liquid synthetic medium for the
707　　　development of mycelial and yeast forms of Candida Albicans. *Sabouraudia* **13**, 148-153
708　　　(1975).
709　64　Spitzer, M., Wildenhain, J., Rappsilber, J. & Tyers, M. BoxPlotR: a web tool for generation
710　　　of box plots. *Nat Methods* **11**, 121-122, doi:10.1038/nmeth.2811 (2014).
711　65　Chaillot, J. *et al.* The Monoterpene Carvacrol Generates Endoplasmic Reticulum Stress in
712　　　the Pathogenic Fungus Candida albicans. *Antimicrob Agents Chemother* **59**, 4584-4592,
713　　　doi:10.1128/AAC.00551-15 (2015).
714　66　Inglis, D. O. *et al.* The Candida genome database incorporates multiple Candida species:
715　　　multispecies search and analysis tools with curated gene and protein information for
716　　　Candida albicans and Candida glabrata. *Nucleic Acids Res* **40**, D667-674,
717　　　doi:10.1093/nar/gkr945 (2012).
718　67　Skrzypek, M. S. *et al.* The Candida Genome Database (CGD): incorporation of Assembly
719　　　22, systematic identifiers and visualization of high throughput sequencing data. *Nucleic*
720　　　*Acids Res* **45**, D592-D596, doi:10.1093/nar/gkw924 (2017).
721　68　Guillemette, T., Sellam, A. & Simoneau, P. Analysis of a nonribosomal peptide
722　　　synthetase gene from Alternaria brassicae and flanking genomic sequences. *Curr Genet*
723　　　**45**, 214-224, doi:10.1007/s00294-003-0479-z (2004).
724　69　Garcia, C. *et al.* The Human Gut Microbial Metabolome Modulates Fungal Growth via
725　　　the TOR Signaling Pathway. *mSphere* **2**, doi:10.1128/mSphere.00555-17 (2017).
726　70　Fonzi, W. A. & Irwin, M. Y. Isogenic strain construction and gene mapping in Candida
727　　　albicans. *Genetics* **134**, 717-728 (1993).
728　71　Saidane, S., Weber, S., De Deken, X., St-Germain, G. & Raymond, M. PDR16-mediated
729　　　azole resistance in Candida albicans. *Molecular microbiology* **60**, 1546-1562,
730　　　doi:10.1111/j.1365-2958.2006.05196.x (2006).
731　72　Dunkel, N., Blass, J., Rogers, P. D. & Morschhauser, J. Mutations in the multi-drug
732　　　resistance regulator MRR1, followed by loss of heterozygosity, are the main cause of
733　　　MDR1 overexpression in fluconazole-resistant Candida albicans strains. *Molecular*
734　　　*microbiology* **69**, 827-840, doi:10.1111/j.1365-2958.2008.06309.x (2008).
735　73　Davis-Hanna, A., Piispanen, A. E., Stateva, L. I. & Hogan, D. A. Farnesol and dodecanol
736　　　effects on the Candida albicans Ras1-cAMP signalling pathway and the regulation of
737　　　morphogenesis. *Molecular microbiology* **67**, 47-62, doi:10.1111/j.1365-
738　　　2958.2007.06013.x (2008).
739
740
741
742
743
744
745
746

747
748 **Figure legends**
749

750 **Figure 1. Hyphal growth inhibition assay in *C. albicans*.**
751 (**A**) Workflow of small-molecule high-throughput screen for hyphal growth inhibition of *C.*
752 *albicans* SC5314 strain. (**B**) Chemical structure of the antifilamentation compound 1 (Cmp #1;
753 N1-(3,5-dichlorophenyl)-5-chloro-2-hydroxybenzamide) and (Cmp #2; 3-Chloro-
754 aryl(benzofuran-2-yl) ketoxime). (**C**) Antifilamentation activity of the Cmp #1 and Cmp #2 at
755 100 µM. *C. albicans* SC5314 strain was grown under hyphae-promoting conditions (SC medium
756 supplemented with 10% FBS) for three hours at 37°C.
757

758 **Figure 2**. **Effect of halogenated salicylanilide analogs on *C. albicans* yeast and hyphal**
759 **growths.**
760 (**A**) Chemical structures of different commercially available salicylanilides. (**B**) Effect of TCSA
761 analogs on both yeast and hyphal growths of *C. albicans*. To assess the effect of each compound
762 on yeast growth at concentrations ranging from 1 to 100µM, *C. albicans* SC5315 strain was
763 grown on SC medium at 30°C for 24 hours. Hyphae-promoting conditions were obtained by
764 incubating *C. albicans* cells on SC medium supplemented with 10 % FBS at 37°C for 3 hours
765 and salicylanilides (1-100µM). (+++), (++) and (+) indicate strong, medium and low inhibition,
766 respectively. Absence of inhibition was indicated by (-).
767

768 **Figure 3**. **Niclosamide and TCSA abolished *C. albicans* hyphal growth promoted by**
769 **different cues.**
770 Effect of Niclosamide (**A**) and TCSA (**B**) on the growth of the commensal yeast form. *C.*
771 *albicans* SC5315 strain was exposed at different concentrations of the two HSA in SC medium
772 and grown at 30°C for 24h. (**C**) Dose-response effect of Niclosamide (**C**) and TCSA (**D**) on
773 filament length of *C. albicans* visualized by box plots. Bold lines in the box plots show the
774 medians. *C. albicans* SC5315 strain was grown under hyphae-promoting conditions (SC + 10%
775 FBS) in the absence (control) or the presence of HSA (10-50µM). Filament length were
776 measured for at least 100 cells and shown as arbitrary unit (AU). (**E-I**) DIC micrographs
777 showing the dose-response antifilamentation effect of Niclosamide and TCSA on *C. albicans*
778 hypha grown on SC medium supplemented with 10% FBS serum (**E**) or on RPMI (**F**), Spider
779 (**G**) and Lee's (**H**) media, and SC with N-acetyl-D- glucosamine (GlcNAc) (**I**).

780 **Figure 4**. **Niclosamide and TCSA antivirulence activity are expanded to the inhibition of**
781 **biofilm formation and host invasion.**
782 Effect of TCSA (**A** and **C**) and Niclosamide (**B** and **D**) on biofilm formation of *C. albicans* (**A-**
783 **B**) and *C. auris* (**C-D**). The effect of HSA on biofilm formation of both *C. albicans* SC5314 and
784 *C. auris* HDQ-RPCau1 strains was assessed using the metabolic colorimetric assay based on the
785 reduction of XTT. Results represent growth inhibition (%) and are shown as the mean of at least
786 three independent replicates. (**E**) Both Niclosamide and TCSA attenuate damage of enterocytes
787 cells caused by *C. albicans*. Damage of the human epithelial intestinal cells HT-29 infected by *C.*
788 *albicans* SC5314 strain was assessed using LDH release assay. Cell damage was calculated as
789 percentage of LDH activity of HSA-treated experiment relatively to that of the control
790 experiment (*C. albicans* invading HT-29 cells in the absence of HSA). Results are represented as
791 the mean of three independent replicates.

18

792 **Figure 5**. **Niclosamide induces retrograde response in** *C. albicans*
793 (**A**) Genome-wide transcriptional profiling reveals that transcript level of genes of anaplerotic
794 reactions are altered in response to Niclosamide. Upregulated and downregulated genes are
795 indicated by red and green, respectively. Transcripts that were not differentially expressed are
796 shown in black. Simplified tricarboxylic and glyoxylate cycles as annotated in the CGD database
797 are shown. (**B-C**) Antifilamentation effect of Niclosamide (**B**) and TCSA (**C**) on *C. albicans*
798 resistant strains with different resistance mechanisms. *C. albicans* 6692 and 5674 resistant strains
799 were grown under hyphae-promoting conditions (SC + 10% FBS) in the absence (control) or the
800 presence of HSA (10-50µM). (**D-E**) Niclosamide and TCSA alter the mitochondrial membrane
801 potential. *C. albicans* SC5314 strain cells were treated with different concentrations (1-50µM) of
802 either TCSA or Niclosamide. Mitochondrial membrane potential ($\Delta\Psi$m) were measured using
803 the fluorescent potentiometric dye JC-1 and flow cytometry (**D**). Alternatively, the effect of both
804 HSA on $\Delta\Psi$m was assessed by MitoTracker staining (**E**). For both of JC-1 and MitoTracker
805 assays, fluorescence ratio and intensities (AU) were presented as the mean of at least three
806 independent experiments.
807
808 **Figure 6**. **Mitochondrial protein import machinery is required for Niclosamide tolerance**
809 **and filamentation.**
810 (**A**) Mining HIP assay data of HSA from studies performed by Hoepfner *et al.* [47] and Corey
811 Nislow' group [48] (http://chemogenomics.pharmacy.ubc.ca/hiphop/) in *S. cerevisiae*. HSA-
812 haploinsufficient mutant hits identified by HIP assay for each compound were selected based on
813 *z*-score ≥ 2.5. The Venn diagram was generated using the web tool software at the following
814 URL: www. bioinformatics.psb.ugent.be/webtools/Venn. (**B**) *C. albicans* heterozygous mutants
815 of the TIM23 complex including *tim23/TIM23*, *tim17/TIM17, tim50/TIM50, ssc1/SSC1* and
816 *mge1/MGE1* are sensitive to high concentration of Niclosamide (200µM). (**C**) The conditional
817 homozygous mutant *mge1/pTeT-MGE1* under repressive conditions (100µg/mL tetracycline) is
818 unable to differentiate true hyphae when grown at 37°C in Spider medium as compared to the
819 parental strain CAI4.
820
821 **Figure 7**. **Chemical genetics of the** *C. albicans* **hyphal signaling network using HSA as**
822 **perturbers.**
823 (**A**) Effect of Niclosamide and TCSA on *C. albicans* mutants overexpressing key regulator of the
824 yeast-to-hyphae transition. Ectopic filamentation of *MAL2p-UME6*, *MAL2p-HGC1ΔC* and
825 *MAL2p-STE11ΔN* mutants was ensured by growing these strains under inducing conditions in
826 YNB- 2% maltose medium at 30°C for 3 hours. (**B**) Constitutive filamentation of the dominant
827 Ras1[G13V] mutant is inhibited by Niclosamide and TCSA. Both Ras1[G13V] mutant and the control
828 strain (CAI4-Ras1) were grown at 30°C on Spider medium.
829
830
831
832
833
834
835
836
837

19

838
839
840   **Table 1**. Gene function and biological process associated with *C. albicans* response to
841   Niclosamide. Gene ontology analysis was performed using the Candida Genome Database GO
842   Term Finder. The *p*-value was calculated using hypergeometric distribution, as described on the
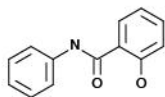843   GO Term Finder website.
844
845

GO category	Gene name	*p*-value[a]
Up-regulated transcripts		
Drug transport	*CDR1, CDR11, QDR3, MDR1, TPO3, MTE4, SGE11,* C1_10710C_A, CR_09830W_A	1.30e-04
Trehalose metabolism in response to stress	*HSP21, NTH1, HSP104, TPS2*	2.10e-02
Glyoxylate metabolic process	*GOR1, ICL1, MLS1,* C4_05390W_A	5.17e-02
Carbohydrate metabolic process	*GAL1, GAL10, TPS2, ICL1, PFK26, MLS1, PFK27, HSP21, GPD1, PYC2, XKS1, NTH1, GSY1, HSP104*	6.25e-02
Oxidation-reduction process	*GOR1, AOX2, ERO1, FMP52, MRF1,* C2_07270W_A, *IFM3, UCF1, GPD1, DAO2, SCS7,* C4_05390W_A, *OYE32, GPX1, OYE23, MIX17, NPD1, ALK2, GSY1, IFE2, CDG1*	7.63e-02
Down-regulated transcripts		
Lipid biosynthetic process	*CWH8, FEN1, LCB2, DGK1, AYR1, ERG6, LAC1, IDI1, PEL1, CYB5, EPT1, COQ1, ERG25, CHO2, NDT80*	1.34e-03
Regulation of protein serine/threonine kinase activity	*RHO2, SOL1, WSC1, PBS2, CLN3, CIP1, CLG1*	7.82e-03
Filamentous growth	*CHS7, RAC1, CAT1, VRG4, SSU81, UTP6, GIN4, NDT80, ESC4, RHO2, RAS1, ASH1, MNT2, CCC1, WSC1, LAC1, MNN9, PBS2, ISW2, CLN3, CHT2, TOP1, CUP9, YEL1, RSR1, SMC5, PGA1*	5.07e-02
Fungal-type cell wall organization or biogenesis	*XOG1, CHS7, RAC1, SSU81, FEN1, SIM1, SPF1, RHO2, MNT2, WSC1, CHS4, MNN9, PBS2, PGA1*	5.99e-02

846
847
848
849
850
851
852

20

853
854
855
856
857
858   **Table 2.** Fungal strains used in this study.
859
860
861
862

Name	Description/Genotype	Reference
Candida albicans		
SC5314 (ATCC-MYA-2876)	*C. albicans* wild-type reference strain.	[70]
5674	Azole-resistant clinical strain (overexpressing the ABC-transporters Cdr1 and Cdr2, and the phosphatidylinositol transfer protein, Pdr16) isolated from mouth	[71]
6692	Azole-resistant clinical strain (overexpressing the MFS-transporter Mdr1 and had a gain-of-function mutation on the transcription factor, Mrr1) isolated from mouth	[71,72]
KC685	*ura3Δ/ura3Δ his1Δ/his1Δ leu2Δ/leu2Δ arg4Δ/arg4Δ pMAL2-URA3*	[16]
KC753	*KC685 STE11/pMAL2- STE11ΔN-URA3*	[16]
KC763	*KC685 UME6/pMAL2-UME6-URA3*	[16]
KC754	*KC685 HGC1/pMAL2- HGC1ΔC-URA3*	[16]
DH545	*ura3::λimm434/ura3 pYPB1-ADHpL-CaRAS1*	[73]
DH409	*ura3::λimm434/ura3 pYPB1-ADHpL-CaRAS1^{G13V}*	[73]
Candida auris		
HDQ-RPCau1	Clinical isolate from Hôtel-Dieu de Québec Hospital, QC, Canada	-

863
864
865
866
867
868
869

A

SC medium + 10% FBS 37°C - 3 hours

678 bioactive compounds

Phenotypic-based screen:
Assay for hyphal growth on the high content microscope Cytation 5

Image analysis and hit identification:
93 small molecules

Pan Assay Intereference Compounds (PAINS):
Exclusion of frequent hitters and promiscuous compounds (43 retained hits)

Growth assay:
Assay for yeast growth on Sunrise-Tecan readers

Selection of compounds that have no or slight effect on the yeast growth (< 5% growth reduction) at 10-1000 µM

Growth (OD)

Time (min)

High priority hits
2 small molecules were retained

B

Cmp #1

Cmp #2

C

Control

Cmp #1 100 µM

Cmp #2 100 µM

A

B

Compound	Name	Effect on yeast growth/filamentation
Comp #3	Salicylanilide (2-Hydroxy-N-phenylbenzamide)	+++/+++
Comp #4	5-bromo-N-(3,5-dichlorophenyl)-2-hydroxy-benzamide	-/+
Comp #5	5-chloro-N-(2,4-difluorophenyl)-2-hydroxy-benzamide	-/+
Comp #6	Niclosamide	-/+++
Comp #7	Oxyclozanide	+++/+++
Comp #8	3,5-dichloro-N-(2,4-difluorophenyl)-4-pyrrol-1-yl-benzamide	-/+
Comp #9	4-amino-3,5-dichloro-N-(3,5-dichlorophenyl)benzamide	+/-
Comp #10	5-chloro-N-(2-chloro-4-nitro-phenyl)-2-hydroxy-benzamide	++/+
Comp #11	Tribromsalan (3,5,4'-Tribromosalicylanilide)	+++/+
Comp #12	Clioxanide	-/+

A Niclosamide

Growth (OD600) vs Concentration (μM): 0, 1, 5, 10, 50, 100

B TCSA

Growth (OD600) vs Concentration (μM): 0, 1, 5, 10, 50, 100

C Niclosamide

Filament lenght (AU) vs Concentration (μM): 0, 10 μM, 20 μM, 30 μM, 40 μM, 50 μM

D TCSA

Filament lenght (AU) vs Concentration (μM): 0, 10 μM, 20 μM, 30 μM, 40 μM, 50 μM

E

	Control	10 μM	20 μM	40 μM	50 μM
Niclosamide					
TCSA					

F

	Control	10 μM	50 μM
TCSA			
Niclosamide			

RPMI

G

	Control	0.5 μM	1 μM
TCSA			
Niclosamide			

Spider

H

	Control	1 μM	5 μM
TCSA			
Niclosamide			

Lee's

I

	Control	0.1 μM	0.5 μM
TCSA			
Niclosamide			

GlcNAc

A — Metabolic pathway diagram

Glutamate

GDH2 (2.67) *GDH3* (0.48)

α–ketoglutarate

TCA cycle

Citrate

Succinate

Oxaloacetate

PYC2 (3.35)

Pyruvate

Acetate

ACS1 1.62

AcetylCoA

Fatty acids

β-oxidation

ALD5 (1.28) *FAA21* (1.49)
ALD6 (1.58) *POT1-2* (1.84)

AcetylCoA

Malate

MDH1-3 (1.40)
MDH1 (1.39)

MLS1 (31.90)

Oxaloacetate

PCK1 (1.85)
FBP1 (1.54)

Glyoxalate cycle

Glyoxalate

Citrate

CIT1

Gluconeogenesis

Succinate

ICL1 (46.25)

Isocitrate

ACO1

B — Niclosamide

Control | 10 μM | 50 μM

SC5314

6692 -*MDR1*^oe

5674 -*CDR1*^oe

Niclosamide

C — TCSA

Control | 10 μM | 50 μM

SC5314

6692 -*MDR1*^oe

5674 -*CDR1*^oe

TCSA

D

Concentration (μM) vs Ratio of red to green fluorescence intensities

☐ Niclosamide ■ TCSA

E

Concentration (μM) vs Mean fluorescence (AU)

☐ Niclosamide ■ TCSA

A

PMA1
1

FOL3
1

MGE1
1

MED6
1

RRB1
1

LSM4
1

Niclosamide

66 1 2 20 29 16 29

B

Control ■ Niclosamide (200 µM) ■

Growth (%)

WT   mge1/MGE1   ssc1/SSC1   tim23/TIM23   tim17/TIM17   tim50/TIM50

C

WT   mge1/pTet-MGE1